

Risedronate Preserves Trabecular Architecture and Increases Bone Strength in Vertebra of Ovariectomized Minipigs as Measured by Three-Dimensional Microcomputed Tomography*

BABUL BORAH, THOMAS E. DUFRESNE, PAULA A. CHMIELEWSKI, GARY J. GROSS,
MARLA C. PRENGER, and ROGER J. PHIPPS

ABSTRACT

Risedronate reduces the risk of new vertebral fractures up to 70% within 1 year of treatment in patients with osteoporosis. Both increases in bone mass and preservation of bone architecture are thought to contribute to antifracture effects. Our objectives were to determine the effects of risedronate on trabecular bone mass and architecture and to determine the relative contributions of mass and architecture to strength in the vertebra of ovariectomized (OVX) minipigs. The minipigs were OVX at 18 months of age and were treated daily for 18 months with either vehicle or risedronate at doses of 0.5 mg/kg per day or 2.5 mg/kg per day. The three-dimensional (3D) bone architecture of the L4 vertebral cores of Sinclair S1 minipigs was evaluated by 3D microcomputed tomography (μ CT). Compared with the OVX control, the vertebral bone volume (bone volume/tissue volume [BV/TV]) was higher in both treated groups ($p < 0.05$). The architectural changes were more significant at the 2.5-mg/kg dose and were more prevalent at the cranial-caudal ends compared with the midsection. At the higher dose, the trabecular thickness (Tb.Th), trabecular number (Tb.N), and connectivity were higher, and marrow space volume (Ma.St.V) and trabecular separation (Tb.Sp) were lower ($p < 0.05$). The trabecular separation variation index (TSVI), a new measure to approximate structural variations, was smaller in the 2.5-mg/kg-treated group ($p < 0.05$). In this group, a significant preservation of trabeculae orthogonal to the cranial-caudal axis was confirmed by a decrease in the degree of anisotropy (DA) and an increase in the percent Cross-strut (%Cross-strut; $p < 0.05$). Both normalized maximum load (strength) and normalized stiffness of the same vertebral cores were higher in the 2.5-mg/kg risedronate group compared with the OVX group ($p < 0.05$). BV/TV alone could explain 76% of the variability of the bone strength. The combination of bone volume and architectural variables explained >90% of the strength. The study showed that risedronate preserved trabecular architecture in the vertebra of OVX minipigs, and that bone strength is tightly coupled to bone mass and architecture. (J Bone Miner Res 2002;17:1139–1147)

Key words: trabecular architecture, osteoporosis, microcomputed tomography, bone strength, risedronate

INTRODUCTION

RISEDRONATE DECREASES the risk of the first new vertebral fracture up to 70% in the first year of treatment in postmenopausal women and in men and women with

glucocorticosteroid-induced osteoporosis.^(1,2) The exact mechanisms for the fracture benefits observed with risedronate and other therapies are not understood fully. Although increased bone mineral density (BMD) clearly contributes to antifracture efficacy, most clinical data show that the relationship between BMD build and fracture reduction is not straightforward. With antiresorptive therapies, the increases in BMD explain only a part of the observed fracture reduction.⁽³⁾ Treatment with two different doses of the bone anabolic agent parathyroid hormone (PTH; 20 μ g everyday

*Presented in part at the 23rd annual meeting of the American Society for Bone and Mineral Research, Phoenix, Arizona, USA, October 12–16, 2001.

All authors are employees of Procter and Gamble Pharmaceuticals.

[q.d.] and 40 μg q.d. for 19 months) produced dose-related increases in BMD (9.7% and 13.7%, respectively) but similar fracture reductions.⁽⁴⁾ However, the fracture reduction provided by PTH treatment was no greater than that provided by 12 months of risedronate treatment with a much smaller increase in BMD ($\sim 4.5\%$) compared with increases observed with PTH. In addition, recent data indicate that prevalent fractures increase the risk of further vertebral fractures independent of bone density.⁽⁵⁾ This evidence suggests that factors besides BMD contribute to bone fragility. Although low bone mass is a major risk factor for fracture, the preservation of trabecular bone architecture is believed to contribute to bone strength and, therefore, to reduction of fracture risk.^(6,7) The improvement in bone architecture has been suggested as contributing to fracture reduction in osteoporotic patients by daily PTH treatment.⁽⁸⁾

In a recent study using three-dimensional (3D) microimaging, we showed that trabecular architecture contributes to compressive strength in the vertebra of growing minipigs over and above that predicted by bone volume or mineral content alone.⁽⁹⁾ The minipig is a remodeling species and has estrous cycles similar to humans. In a previous pilot study in Sinclair S1 minipigs, the combination of ovariectomy and calcium-restricted diet induced bone changes similar to those seen in postmenopausal osteoporosis, resulting in loss of bone, trabecular architecture, and strength.⁽¹⁰⁾ These characteristics make it a suitable large animal model to be used in the nonclinical evaluation of the effects of therapies on bone loss, architecture, and strength.

In this safety and efficacy study, Sinclair S1 minipigs were ovariectomized (OVX) and were treated with risedronate for 18 months. We analyzed vertebral samples to investigate the effect of risedronate on the 3D architectural and biomechanical properties of the vertebra. Some data on the risedronate effects on BMD and conventional histomorphometry in this study are presented elsewhere.^(11,12)

The objectives of our analyses were to derive architectural descriptors of the lumbar spine vertebral specimens of the OVX minipigs using 3D microcomputed tomography (μCT) to assess the effects of daily treatment with risedronate on trabecular architecture, evaluate the effect of risedronate treatment on vertebral compressive strength, and assess the relative contribution of trabecular bone volume and 3D architecture to compressive strength of the same specimens.

MATERIALS AND METHODS

Samples

Sinclair S1 female minipigs (Sinclair Research Center, Columbia, MO, USA) were fed a calcium-restricted (0.75%) diet from 4 months of age and were OVX or sham-operated at ~ 18 months of age, before initiation of treatment. All animals were maintained on the calcium-restricted diet throughout the study. Risedronate was administered in a vehicle of 65% sucrose at doses of 0.05, 0.1, 0.5, and 2.5 mg/kg per day orally.^(11,12) Calcium-restricted sham and OVX control groups were given 65% sucrose vehicle daily for 18 months. Dosing was initiated within 2–3 weeks

after surgery. After necropsy, L4 vertebral cores were prepared from all animals. For this study on vertebral trabecular architecture (using μCT) and strength, we analyzed the L4 vertebral cores from four study groups: OVX control ($n = 11$), sham ($n = 11$), 0.5 mg/kg of risedronate ($n = 11$), and 2.5 mg/kg of risedronate ($n = 10$). To prepare vertebral cores, the dorsal and the ventral cortical surfaces from each L4 vertebral body were removed with a precision band saw producing a central slab ~ 7 mm thick, which was trimmed to remove any residual lateral and medial cortices. The resulting slabs included both intact epiphyses and epiphyseal plates. After trimming, samples were stored in 70% ethanol.

μCT

A μCT scanner ($\mu\text{CT}20$; Scanco Medical AG, Basserdorf, Switzerland)⁽¹³⁾ was used for 3D imaging. The scanner was checked weekly for accuracy and precision during the study using custom-made phantoms as previously described.⁽¹⁴⁾ For image acquisition, a vertebral specimen was placed in a 17-mm holder and imaged in the cranial-caudal direction of the intact core. The 3D images consisted of ~ 1000 2D slices (300 projections; 512×512 data matrix) at a $34\text{-}\mu\text{m}$ voxel size in all three axes. Typical scanning time was 18–24 h per specimen. During acquisition, the vertebral samples were kept moist in 70% ethanol. After image acquisition, the 3D data set was transferred to a Silicon Graphics Onyx II computer (Silicon Graphics, Mountain View, CA, USA) and was presented as an 8-bit binary gray level image. A fixed threshold of 60 (0–255 range) was used to separate the bone from the background, creating a bilevel image. A mask of the entire trabecular region was created to insure that only the trabecular region was evaluated. The cortical bone was separated from trabecular bone using an automated algorithm.⁽¹⁵⁾

Determination of 3D trabecular architecture

A spatial preference for architectural changes in the trabecular bone under the end plates, with relative sparing of the midsection of the vertebra has been reported previously for OVX minipigs.⁽¹⁶⁾ Therefore, for architecture analysis, the trabecular region was divided digitally into three distinct regions consisting of the midregion (middle 50%) and the cranial and caudal ends (each 25% of the trabecular volume; Fig. 1). For comparisons with the biomechanical properties, the architecture values were averaged over the entire trabecular region.

The following measurements were included:

Bone Volume/Tissue Volume (BV/TV, %) and Bone Surface/Tissue Volume (BS/TV, 1/mm) were estimated using standard procedures.⁽¹⁷⁾

Trabecular thickness (Tb.Th), trabecular separation (Tb.Sp), and trabecular number (Tb.N) were measured by direct method, which is independent of an underlying model, as well as derived assuming a plate model. Direct Tb.Th (Tb.Th-direct, μm) was calculated as the average diameter of the largest nonoverlapping spheres that fit inside

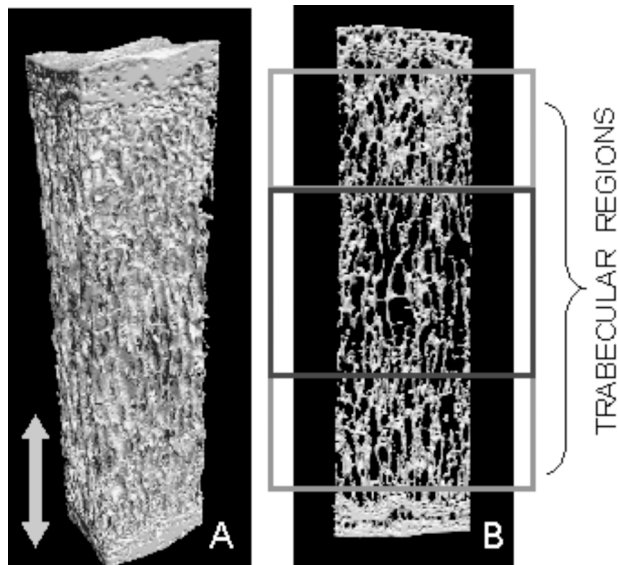


FIG. 1. (A) A surface-rendered 3D μ CT image of a minipig vertebral core (arrow points along the cranial-caudal axis). (B) Architecture analysis was performed on three digitally divided trabecular regions consisting of the midregion (middle 50%) and the cranial and caudal ends (each 25% of the trabecular volume).

the trabecular bone throughout the volume of interest (VOI).⁽¹⁸⁾ Direct Tb.Sp (Tb.Sp-direct, μ m) was measured using the average diameter of the largest nonoverlapping spheres that fit inside the marrow space throughout the VOI.⁽¹⁹⁾ Direct Tb.N (Tb.N-direct, 1/mm) is the inverse of the diameter of the largest nonoverlapping spheres that fit inside the marrow space where the trabecular bone is only represented by its centerline.⁽¹⁹⁾

The derived indices of Tb.Th (Tb.Th-derived), Tb.Sp (Tb.Sp-derived), and Tb.N (Tb.N-derived) were calculated from bone volume and bone surface area.⁽¹⁷⁾ Trabecular separation variation index (TSVI) is a new measure that approximates the variations of marrow space thickness. The direct method for Tb.Sp yielded both an average value and an SD across VOI. TSVI was defined as the SD of Tb.Sp distribution and provided an independent measure of structural variability. TSVI was log-transformed for statistical analysis so that it better approximates normality.

Connectivity density (ConnD, mm^{-3}) is a topological parameter that estimates the number of trabecular connections per cubic millimeter. The perforations of plates without the breaking of trabecular connections would artificially inflate ConnD.⁽¹⁶⁾ Therefore, in our calculation, a stepwise dilation of the bone voxels was used to remove the holes, thereby minimizing the contribution from perforations. After a three-step dilation, the ConnD was derived from the Euler number.⁽²⁰⁾

Marrow star volume (Ma.St.V, mm^3), described previously in 2D histomorphometry,⁽²¹⁾ is a measure of the "voids" within the trabecular structure and was extended to the third dimension.⁽⁹⁾

Degree of anisotropy (DA) defines the direction and magnitude of preferred orientation of trabeculae. The higher

the DA, the more the bone is aligned with the principal axis relative to the other axes. It was calculated as the ratio between the maximal and minimal radii of the mean intercept length (MIL) ellipsoid.^(22,23)

Percent Cross-strut (%Cross-strut) is the amount of trabeculae in planes orthogonal to the load direction. It assumes a priori knowledge of the major loading direction (cranial-caudal for minipig) and was calculated as $100 - \% \text{Bone}_{\text{load direction}}$.⁽²⁴⁾

Percent Plate (%Plate) is a new parameter developed to quantify a relative estimate of plates and is estimated by comparing the direct and derived (plate or rod model) thickness.⁽²⁴⁾ It is calculated as

$$\% \text{Plate} = 1 - \left\{ \left(\frac{\text{thickness}_{\text{direct}} - \text{thickness}_{\text{plate model}}}{\text{thickness}_{\text{rod model}} - \text{thickness}_{\text{plate model}}} \right) \right\} * 100.$$

Biomechanical testing

After μ CT acquisition, the samples of the OVX group and the risedronate, 2.5 mg/kg, group were used for biomechanical compression testing. Before mechanical testing, the epiphyseal ends were trimmed to provide flat ends for adhering to test platens. The cross-sectional areas at the two sample ends and at the midpoint were measured and averaged over all three locations. A single measurement of sample height was taken and recorded. Average sample dimensions (\pm SD) were 25.00 mm (\pm 0.86), 8.88 mm (\pm 2.33), and 7.44 mm (\pm 1.63) for height, width, and thickness, respectively. These measurements of geometry were used to normalize the mechanical property data to provide values of bulk properties. For compression testing, the distal ends of each biopsy specimen were secured to cylindrical acrylic blocks using cyanoacrylate glue to reduce errors due to end effects.⁽²⁵⁾ Samples were placed in custom compression fixtures attached to a servohydraulics testing machine (Instron model 8511; Instron Corp., Canton, MA, USA) and were compressed along the cranial-caudal direction with a uniform displacement rate of 4 mm/s until failure using a 5-kN load cell and approximate preload of 26 newtons (N). The data from one sample of the placebo group were discarded, because the preloading step did not automatically stop at the required threshold.

The maximum load was quantified as the highest value of force encountered before failure and normalized by dividing by the average cross-sectional area. The normalized stiffness, which reflects the sample's resistance to strain, was calculated as the slope of the tangent line of the initial linear region of the stress-strain curve.

Statistical analysis

A two-sample *t*-test or an analogous nonparametric method (Wilcoxon rank sum test) was used to compare the different treatment groups. Multiple linear regressions (MLRs) were used to model normalized maximum load and normalized stiffness using the structural parameters as in-

TABLE 1. THE GROUP MEAN (SD) OF BV AND TRABECULAR ARCHITECTURAL PARAMETERS OF CRANIAL-CAUDAL ENDS AND MIDSECTIONS FOR THE SHAM, OVX, AND RISEDRONATE (RIS)-TREATED GROUPS

Parameters	Sham		OVX		RIS (0.5 mg)		RIS (2.5 mg)	
	Ends	Middle	Ends	Middle	Ends	Middle	Ends	Middle
BV/TV (%)	30.62 (2.64)	26.40 (3.27)	29.64 (3.30)	25.43 (3.59)	32.35* (2.14)	28.29* (1.85)	33.68* [†] (4.19)	30.96* [†] (3.99)
BS/TV (1/mm)	4.64 (0.37)	4.08 (0.55)	4.58 (0.32)	4.01 (0.32)	4.78 (0.26)	4.16 (0.32)	5.01* [†] (0.57)	4.32 (0.45)
Tb.Th-direct (μ m)	144.6 (7.84)	145.55 (11.42)	142.5 (11.07)	143.43 (10.57)	148.45 (9.56)	153.06 (13.1)	146.65 (8.82)	158.79* (8.59)
Tb.Th-derived (μ m)	132.19 (8.01)	129.99 (9.89)	129.56 (12.86)	126.76 (13.16)	135.54 (8.73)	136.37* (9.55)	134.84 (11.5)	143.38* [†] (10.55)
Tb.Sp-direct (μ m)	474.86 (57.02)	596.99 (147.07)	472.01 (42.33)	579.48 (65.3)	439.4 (31.07)	553.91 (59.27)	403.76* (62.58)	521.75 (82.89)
Tb.Sp-derived (μ m)	301.68 (34.26)	369.41 (70.13)	309.02 (30.88)	375.15 (43.74)	284.03 (20.89)	346.80 (32.16)	269.44* [†] (45.08)	324.49* (50.39)
Tb.N-direct (1/mm)	2.10 (0.21)	1.75 (0.31)	2.05 (0.18)	1.71 (0.15)	2.18 (0.19)	1.79 (0.23)	2.38* (0.29)	1.92* (0.24)
Tb.N-derived (1/mm)	2.32 (0.18)	2.04 (0.28)	2.29 (0.16)	2.00 (0.16)	2.39 (0.12)	2.08 (0.16)	2.50* [†] (0.28)	2.16 (0.22)
ConnD (1/mm ³)	2.93 (0.99)	2.74 (1.04)	3.16 (0.98)	2.84 (0.90)	3.33 (0.60)	3.05 (0.49)	4.34* [†] (1.63)	3.22 (1.01)
Ma.St.V (mm ³)	3.65 (1.45)	8.50 (8.10)	4.07 (1.45)	7.61 (3.10)	2.88* (0.75)	5.70 (1.98)	2.57* (1.36)	5.04 (2.37)
DA	2.28 (0.17)	2.22 (0.16)	2.39 (0.19)	2.37 (0.27)	2.26 (0.12)	2.18* (0.15)	2.19* (0.14)	2.09* (0.15)
%Cross-strut	31.70 (3.34)	32.64 (3.42)	30.24 (3.90)	31.01 (4.63)	31.41 (2.01)	32.14 (2.15)	33.54* (3.04)	34.73* (3.03)
%Plate	69.07 (2.70)	67.83 (3.12)	67.74 (4.68)	66.56 (4.81)	69.68 (2.78)	69.06 (2.66)	68.51 (4.46)	69.98* (3.21)
TSVI	2.17 (0.09)	2.38 (0.17)	2.14 (0.04)	2.36 (0.14)	2.11* (0.04)	2.37 (0.13)	2.08* [†] (0.07)	2.36 (0.13)

The direct and derived measures of Tb.Th, Tb.N, and Tb.Sp had strong intraparameter correlation (R^2 between 0.82 and 0.91). TSVI is the SD of Tb.Sp-direct and was log-transformed for all analyses.

* Significantly different from OVX, $p \leq 0.05$; [†] Significantly different from sham, $p \leq 0.05$.

dependent variables. The regression analysis produced a coefficient of multiple determination R^2 , which represents the proportion of variability in the dependent parameter explained by the structural parameters in the model. All results were assessed at the 0.05 significance level.

RESULTS

Effects on bone volume and trabecular architecture

The architectural measurements are presented in Table 1. In comparison with the sham group, ovariectomy reduced BV/TV, although the effects were not significant. BV/TV was significantly higher in the two risedronate doses compared with the OVX group at both regions. The 2.5-mg/kg risedronate dose induced greater but not significant changes in bone volume relative to the 0.5-mg/kg dose.

Representative 3D μ CT images (Fig. 2) of the L4 vertebra of OVX and risedronate-treated (2.5 mg/kg) minipigs illustrate the architectural changes. Visually, the trabecular bone is thicker and the trabecular separations are narrower

in the risedronate-treated animals. Compared with the OVX control animals, treatment-related differences in architecture were found to be region specific and more significant in the 2.5-mg/kg group (Table 1). For the average of the two ends, the following changes were significantly different from OVX controls for the 2.5-mg/kg group: Tb.N (direct and derived) and ConnD increased whereas Tb.Sp (direct and derived), TSVI, and Ma.St.V decreased. For the mid-section, the following changes were significantly different from OVX for the 2.5-mg/kg group: Tb.Th (direct and derived), Tb.N (direct), and %Plate increased, whereas Tb.Sp (derived) decreased (Table 1).

As revealed by the μ CT images (Fig. 3), the relative amount of trabecular bone orthogonal to the cranial-caudal axis (colored in blue) was higher in the vertebra of the risedronate-treated animal compared with the OVX animal. This observation was confirmed quantitatively by a significant increase in the %Cross-strut, and a concomitant significant decrease in the average DA in the risedronate, 2.5 mg/kg, group compared with the OVX controls (Table 1 and Fig. 3).

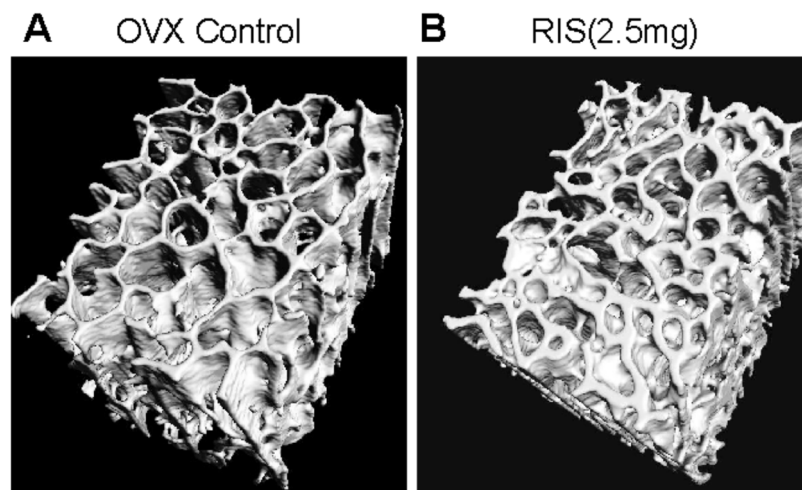


FIG. 2. A comparison of the 3D surface-rendered μ CT images of minipig vertebral cores of (A) an OVX control and (B) a risedronate-treated (2.5 mg/kg per day) animal.

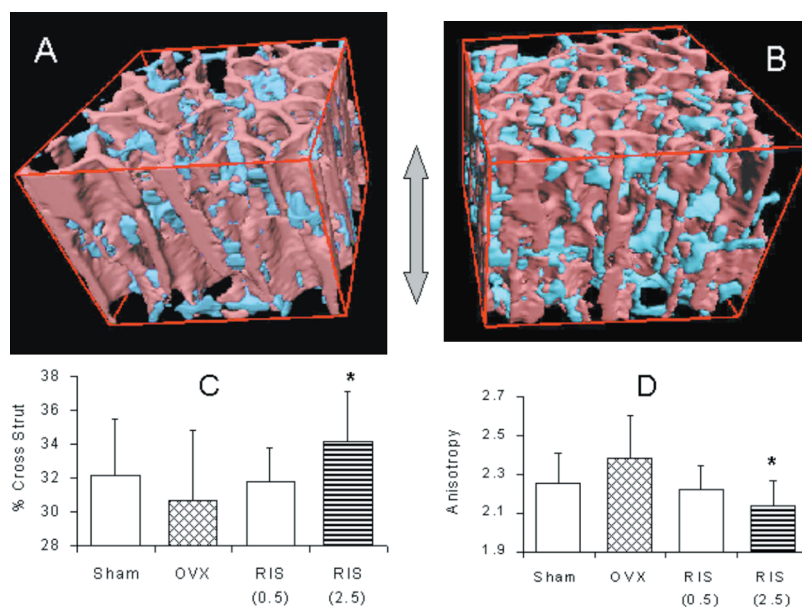


FIG. 3. (A and B) The visualization of cross-struts (trabecular bone orthogonal to the load direction, shown in blue) in the 3D μ CT images of the vertebra in (A) an OVX control and (B) a treated (2.5 mg/kg of risedronate) minipig. (C and D) Plots of group differences in (C) %Cross-strut and (D) DA for the sham, OVX control, and risedronate (RIS) (0.5 mg/kg and 2.5 mg/kg) groups ($p < 0.05$). *Significantly different from the OVX group.

Comparing the 0.5-mg/kg risedronate group with the OVX control, the following region-specific changes were significant: Tb.Th-derived increased whereas DA, Ma.St.V, and TSVI all decreased (Table 1).

Comparing the risedronate, 2.5 mg/kg group, to the sham group, BV/TV increased in both regions, and there were region-specific increases in Tb.N-direct, Tb.Th-derived, and ConnD and region-specific decreases in Tb.Sp-derived and TSVI (Table 1).

Biomechanical measurements

Both normalized maximum load (strength) and normalized stiffness were significantly higher in the risedronate, 2.5 mg/kg, group than in the OVX group (Fig. 4). The means (SD) of the maximum load (strength) for the OVX and 2.5-mg/kg treatment groups were 24.1 (5.3) MPa and 29.8 (5.5) MPa, respectively. The means (SD) of stiffness

for these treatment groups were 1359.3 (163.6) MPa and 1672.8 (239.2) MPa, respectively.

Correlations between architecture and biomechanical properties

To understand how architectural measures jointly affect bone strength, MLR models were used. In these models, we considered the combined effects of two or more architectural parameters in their ability to explain bone strength (Table 2). In a simple linear regression model, BV/TV showed a strong correlation with normalized maximum load ($R^2 = 0.76$), meaning that bone volume explained 76% of the variance in strength. Several architectural parameters individually showed a moderate to strong correlation with maximum load, with Tb.Th-direct having the strongest relationship ($R^2 = 0.63$). Better prediction of the strength was

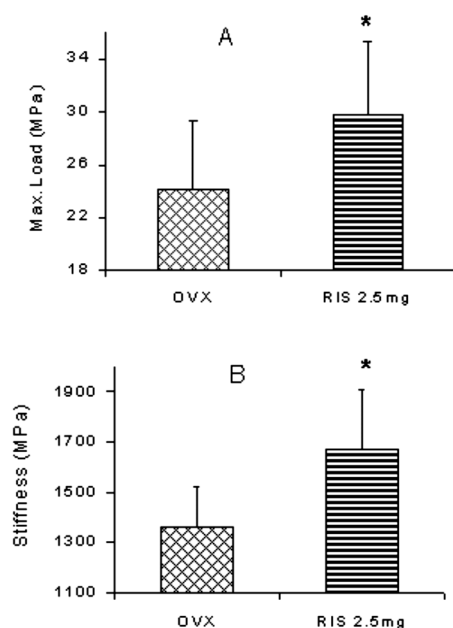


FIG. 4. Plots of group differences in (A) normalized maximum load (MPa) and (B) normalized stiffness (MPa) for the OVX and the 2.5-mg/kg RIS groups ($p < 0.05$). *Significantly different from the OVX.

obtained using MLR with two architectural parameters. Using this model, TSVI and Tb.Th-direct had the highest correlation ($R^2 = 0.84$). In the three-parameter MLR models, where BV/TV was forced to be one of the three parameters, the R^2 increased to as high as 0.91.

When modeling normalized stiffness, BV/TV had an $R^2 = 0.49$ in a simple linear regression analysis; the two-parameter model with TSVI and Tb.Th-direct had an $R^2 = 0.62$. The three-parameter models did not provide further improvement.

DISCUSSION

This is the first study reporting the effects of an antiresorptive agent on trabecular BV and trabecular 3D architecture and their relative contributions to biomechanical strength measured in the same vertebral specimens of a large, bone-remodeling species.

Effect of ovariectomy

In this study, the bone volume and architectural indices measured by μ CT did not change significantly in the OVX group compared with the sham group, although other indices (BMD and histomorphometry) did show some evidence of bone loss after ovariectomy.⁽¹²⁾ In addition, ovariectomy with a mild calcium-restricted diet has been shown to elevate bone turnover in a previous study in minipigs.⁽¹⁰⁾ This apparent lack of effect of ovariectomy seen on μ CT analysis of this study should be considered in light of growth-related changes in bone volume and architecture. Minipigs reach peak bone mass by about 3 years of age,⁽²⁶⁾ and we have

TABLE 2. R^2 VALUES OF SIMPLE AND MLR ANALYSES BETWEEN NORMALIZED MAXIMUM LOAD AND STRUCTURAL PARAMETERS

Model	Structural parameters	R^2
One parameter	BV/TV	0.76
	Tb.Th-direct	0.63
Two parameters	TSVI + Tb.Th-direct	0.84
	Tb.Sp-derived + Tb.Th-derived	0.83
	Tb.Th-derived + Ma.St.V	0.83
Three parameters	BV/TV + TSVI + DA	0.84
	BV/TV + TSVI + ConnD	0.87
	BV/TV + TSVI + %Plate	0.87
	BV/TV + TSVI + Tb.N	0.91

R^2 , the coefficient of multiple determination, represents the proportion of the variability of the maximum load explained by BV and average architectural parameters in the model.

previously shown that vertebral architecture changes significantly during the growth period.⁽⁹⁾ The minipigs used in the study were 18 months old at the time of ovariectomy and initiation of treatment, and therefore were in the growing phase during the course of the study. Growth-related increases in trabecular BV and associated changes in architecture likely countered any loss of bone mass and structure due to ovariectomy.

Effect of risedronate

Treatment with risedronate (0.5 mg/kg daily and 2.5 mg/kg daily) produced significantly higher BV/TV in all regions in the L4 vertebra relative to the OVX minipigs. At the higher dose, the higher trabecular bone volume resulted from increased Tb.Th and Tb.N with concomitant decrease in Ma.St.V and Tb.Sp. In contrast, previous studies with alendronate treatment in adult baboons⁽²⁷⁾ and pamidronate treatment in adult dogs⁽²⁸⁾ found that bone volume increased because of an increase in Tb.Th without changes in connectivity or Tb.N. Several factors could have contributed to this difference between our results and those of other bisphosphonate studies. This study used skeletally immature minipigs while the other studies used skeletally mature animals, causing differences in age-related changes in architecture. Although the other studies used conventional 2D histomorphometric analysis, the 3D measurements in our study were evaluated using the entire biopsy specimen, thereby reducing sampling errors. In addition, differences in relative antiresorptive potencies and exact mechanism of action might contribute to differential effects on bone remodeling. Risedronate, a pyridinyl bisphosphonate, showed higher antiresorptive potency in preclinical studies than either alendronate or pamidronate, both of which are primary amines.⁽²⁹⁾

Significant structural differences were observed between the risedronate, 2.5 mg/kg, group and the sham group. The bone volume increased significantly at both ends and mid-sections and the 3D architecture was altered with risedronate, 2.5 mg/kg. A possible explanation is that the antire-

sorptive action in these young growing animals resulted in increased retention of primary spongiosa and/or in a positive bone balance at remodeling sites.⁽³⁰⁾

On a milligram per kilogram basis, the doses of 0.5 mg/kg per day and 2.5 mg/kg per day of risedronate are higher than approved clinical doses (~5–30 times the osteoporosis clinical dose of 5 mg daily). However, pharmacokinetic data are not available; therefore, it is not possible to compare systemic exposures in this study to exposure produced by clinical doses. The 0.5-mg/kg per day dose reduced vertebral bone turnover by ~50%,⁽¹¹⁾ similar to the reduction in bone turnover produced by long-term treatment with 5 mg daily in osteoporosis.⁽³¹⁾ Therefore, it seems likely that these doses represent one to five times the clinical 5-mg dose based on systemic exposure.

Architecture and strength

In this study, the nondestructive imaging by μ CT allowed for biomechanical testing of the same specimens for direct comparison of bone strength and architecture, making the correlative studies more meaningful. The results indicate that architecture is coupled to the mechanical properties of bone. BV/TV, which is a surrogate measure of density, explained ~76% of vertebral strength, which was in agreement with the results of our previous study with growing minipigs⁽⁹⁾ and with other reports in the literature.^(32,33) As shown in Table 2, in a two-parameter model, architectural parameters alone improved correlation with strength up to 84%. By supplementing BV/TV with different combinations of architectural parameters in a three-parameter MLR model, the prediction of strength data improved to 86–91%. Several of these parameters, such as connectivity, anisotropy, and %Plate have no direct relationship to bone volume, suggesting independent architectural contribution to bone strength. It also is interesting to note that the TSVI appeared in several combinations of the MLR analysis (Table 2). TSVI approximates the variability of marrow space thickness or void volume in 3D, and as such represents the uniformity in trabecular spacing. A significantly smaller TSVI indicated more structural uniformity in the 2.5-mg/kg risedronate-treated vertebra. Engineering principles indicate that structural uniformity should lead to a more uniform distribution of load and stronger material. Therefore, it is not surprising that the inclusion of TSVI in the models improved the architecture to strength correlation. Overall, the results showed that 3D architecture made additional contributions to compressive strength in the minipig vertebra, and that the combination of bone volume and architecture correlated with strength better than did bone volume alone. Although the contribution of trabecular architecture to bone strength was small in these minipigs, it should be noted that bone volume was high (25–33%). Architecture is likely to contribute more to bone strength and fracture risk in low bone mass conditions such as in women with osteoporosis.^(34,35) Our results are consistent with previous work by other investigators that the prediction of mechanical properties of human trabecular bone can be improved if architectural indices are added to the bone volume measurements.⁽³⁴⁾ The data from this study reiterate

the limitation of bone volume or bone mass as a surrogate marker of bone strength.

The correlation between normalized stiffness and structural parameters was lower probably because of the sensitivity of stiffness calculations to specimen characteristics, including dimensions, end effects, and variation in aspect ratios. The samples were of different heights, which may have allowed for different strain patterns and total deformations. In addition, the sample ends were not embedded and therefore errors associated with end effects⁽²⁵⁾ could not be ruled out completely.

Cross-struts in minipigs: functional similarity to horizontal trabeculae in humans

In quadruped mammals, the spine is able to transfer vertical body weight forces into longitudinal compressive forces aligned along the vertebral column with its predominant loading vector in the cranial-caudal direction.⁽³⁶⁾ The function of the cross-struts, which are orthogonal to the loading axis, may be twofold: resisting radial stresses and preventing the longitudinal trabeculae from buckling. There is functional similarity between the cross-struts in minipig vertebra and the horizontal trabeculae in the human vertebra. In the human, the trabecular structure consists of vertical plates along the load direction and supporting horizontal struts. A reduction in cross-sectional area occupied by the horizontal struts may cause a reduction in vertebral strength and follows from Euler Buckling theory.⁽³⁷⁾ As studies have shown, it is the predominant disappearance of the horizontal struts that lead to reduced load-bearing capacity in the human vertebrae.⁽³⁸⁾ Therefore, the preservation of trabecular architecture is paramount to preserving vertebral strength and reducing the risk of fractures. In this study, the number of cross-struts in the 2.5-mg/kg risedronate group was visually higher compared with the OVX group (Fig. 3) and is quantitatively confirmed by a decrease in DA ($p \leq 0.05$) and an increase in %Cross-strut ($p \leq 0.05$). These measurements, when taken together, show that risedronate treatment significantly preserved cross-struts in the minipig vertebrae, which resulted in higher connectivity and Tb.N.

Recently, risedronate was shown to be effective in preserving trabecular architecture in the iliac crest of postmenopausal women who were at risk of osteoporotic fractures.⁽³⁹⁾ Although there is no direct corollary between these minipig results and the human findings, our results suggest that the preservation of trabecular architecture by risedronate could produce stronger bone and thereby contribute to a greater reduction in fracture risk than would be expected based on the increase in bone mass alone.

In conclusion, our work shows that risedronate preserves the 3D trabecular architecture in the vertebra of calcium-deficient OVX minipigs, a large, bone-remodeling species. Biomechanical analysis showed that these changes in architecture contribute to stronger bone, which may help explain the antifracture efficacy of risedronate observed in clinical trials.

ACKNOWLEDGMENTS

The authors thank Dr. Michael Manhart, Dr. Earl Sod, and Dr. Nora Zorich for critically reading this study and Katie Combs for her assistance in biomechanical sample testing. We acknowledge Lisa Bosch for an excellent job in editing this article.

REFERENCES

1. Reginster J-Y, Minne HW, Sorensen OH, Hooper M, Roux C, Brandi ML, Lund B, Ethgen D, Pack S, Roumagnac I, Eastell R 2000 Randomized trial of the effects of risedronate on vertebral fractures in women with established postmenopausal osteoporosis. *Osteoporos Int* **11**:83–91.
2. Reid DM, Hughes RA, Laan Ronald FJM, Sacco-Gibson NA, Wenderoth DH, Adami S, Eusebio RA, Devogelaer J-P 2000 Efficacy and safety of daily risedronate in the treatment of corticosteroid-induced osteoporosis in men and women: A randomized trial. *J Bone Miner Res* **15**:1006–1013.
3. Watts N, Bockman R, Smith C, Li Z, Eastell R, Pack S, Lindsay R 2000 BMD changes explains only a fraction of the observed fracture risk reduction in risedronate-treated patients. *Osteoporos Int* **1**(Suppl 2):S46.
4. Neer RM, Arnaud DC, Zanchetta JR, Prince R, Gaich GA, Reginster J-Y, Hodsman AB, Eriksen EF, Ish-Shalom S, Genant HK, Want O, Mitlak BH 2001 Effect of parathyroid hormone (1-34) on fractures and bone mineral density in postmenopausal women with osteoporosis. *N Engl J Med* **344**:1434–1441.
5. Lindsay R, Silverman SL, Cooper C, Hanley DA, Barton I, Broy SA, Licata A, Benhamou L, Geusens P, Flowers K, Stracke H, Seeman E 2001 Risk of new vertebral fracture in the year following a fracture. *JAMA* **285**:320–323.
6. Parfitt AM 1992 Implications of architecture for the pathogenesis and prevention of vertebral fracture. *Bone* **13**:S41–S47.
7. Kleerekoper M, Villanueva AR, Stanciu J, Rao DS, Parfitt AM 1985 The role of three-dimensional trabecular microstructure in the pathogenesis of vertebral compression fractures. *Calcif Tissue Int* **37**:594–597.
8. Dempster DW, Cosman F, Kurland ES, Zhou H, Nieves J, Woelfert L, Shane E, Plavetic K, Muller R, Bilezikian J, Lindsay R 2001 Effects of daily treatment with parathyroid hormone on bone microarchitecture and turnover in patients with osteoporosis: A paired biopsy study. *J Bone Miner Res* **16**:1846–1853.
9. Borah B, Dufresne TE, Cockman MD, Gross GJ, Sod EW, Myers WR, Combs KH, Higgins RE, Pierce SA, Stevens ML 2000 Evaluation of changes in trabecular bone architecture and mechanical properties of minipig vertebrae by three-dimensional magnetic resonance microimaging and finite element modeling. *J Bone Miner Res* **15**:1786–1797.
10. Moskilde L, Weisbrode SE, Safran JA, Stills HF, Jankowsky ML, Ebert DC, Danielsen CC, Sogard CH, Franks AF, Stevens ML, Paddock CL, Boyce RW 1993 Evaluation of the skeletal effects of combined mild dietary restriction and ovariectomy in Sinclair S-1 minipigs: A pilot study. *J Bone Miner Res* **8**:1311–1321.
11. Gropp KE, Bouchard GF, Phipps RJ, Smith PN 1997 Risedronate dose-dependently decreases bone turnover in ovariectomized minipigs. *J Bone Miner Res* **12**:S1;S471.
12. Phipps R, Mackey M, Raimondi K, Myers W, McOsker J, Bouchard G 1996 Risedronate treatment prevents ovariectomy-induced changes in bone mineral density of lumbar vertebrae in minipigs. *Osteoporos Int* **6**(Suppl 1):257.
13. Ruegsegger P, Koller B, Muller R 1996 A microtomographic system for the nondestructive evaluation of bone architecture. *Calcif Tissue Int* **58**:24–29.
14. Chmielewski PA, Dufresne TE, Combs KH, Borah B, Lundy MW 2001 Validation of a micro-CT system for the 3-D measurement of bone. *J Bone Miner Res* **16**:S1;S461.
15. Dufresne TE 1998 Segmentation techniques for analysis of bone by three-dimensional computed tomographic imaging. *Technol Health Care* **6**:351–359.
16. Boyce RW, Ebert DC, Youngs TA, Paddock CL, Mosekilde L, Stevens ML, Gundersen HJ 1995 Unbiased estimation of vertebral trabecular connectivity in calcium-restricted ovariectomized minipigs. *Bone* **16**:637–642.
17. Feldkamp LA, Goldstein SA, Parfitt AM, Jesion G, Kleerekoper M 1989 The direct examination of three-dimensional bone architecture in vitro by computed tomography. *J Bone Miner Res* **4**:3–11.
18. Hildebrand T, Ruegsegger P 1997 A new method for the model-independent assessment of thickness in three-dimensional images. *J Microsc* **185**:67–75.
19. Hildebrand T, Laib A, Muller R, Dequeker J, Ruegsegger P 1999 Direct three-dimensional morphometric analysis of human cancellous bone: Microstructural data from spine, femur, iliac crest, and calcaneus. *J Bone Miner Res* **14**:1167–1174.
20. Odgaard A, Gundersen HJ 1993 Quantification of connectivity in cancellous bone, with special emphasis on 3-D reconstructions. *Bone* **14**:173–182.
21. Vesterby A 1993 Marrow space star volume can reveal change of trabecular connectivity. *Bone* **14**:193–197.
22. Harrigan TP, Mann RW 1984 Characterization of microstructural anisotropy in orthotropic materials using a second rank tensor. *J Mater Sci* **19**:761–767.
23. Ulrich D, Rietbergen van B, Laib A, Ruegsegger P 1999 The ability of three-dimensional structural indices to reflect mechanical aspects of trabecular bone. *Bone* **25**:55–60.
24. Borah B, Gross GJ, Dufresne TE, Smith TS, Cockman MD, Chmielewski PA, Lundy MW, Hartke JR, Sod EW 2001 Three-dimensional microimaging (MR μ I and μ CT), finite element modeling and rapid prototyping provide unique insights into bone architecture in osteoporosis. *Anat Rec (New Anat)* **265**:101–110.
25. Guo XE, Gibson LJ, McMahon TA 1993 The fatigue of trabecular bone: Avoiding end-crushing artifacts. *Transactions of the 39th Meeting of the Orthopedic Research Society, San Francisco, CA, USA*, p. 584.
26. Bouchard GF, Durham HE, McOsker JE, Krause GF, Eversieck MR, Reddy CS 1995 Determination of the peak bone mass and whole body composition in Sinclair miniature swine. *J Bone Miner Res* **10**:S1;T488.
27. Balena R, Toolan BC, Shea M, Markatos A, Myers ER, Lee SC, Opas EE, Seedor JG, Klein H, Frankenfield D 1993 The effects of 2-year treatment with aminobisphosphonate alendronate on bone metabolism, bone histomorphometry and bone strength in ovariectomized nonhuman primates. *J Clin Invest* **92**:2577–2586.
28. Grynepas MD, Acito A, Dimitriu M, Mertz BP, Very JM 1992 Changes in bone mineralization, architecture and mechanical properties due to long-term (1 year) administration of pamidronate (APD) to adult dogs. *Osteoporos Int* **2**:74–81.
29. Geddes AD 1994 Bisphosphonates: Structure-activity relationships and therapeutic implications. *Bone Miner Res* **8**:265–306.
30. Boyce RW, Wronski TJ, Ebert DC, Stevens ML, Paddock CL, Youngs TA, Gundersen HJ 1995 Direct stereological estimation of three-dimensional connectivity in rat vertebrae: Effect of estrogen, etidronate and risedronate following ovariectomy. *Bone* **16**:209–213.
31. Eriksen E, Melson F, Brown J, Sacco-Gibson N, Balena R, Sod E, Axelrod D, Chines A 1999 Three years of risedronate treatment significantly decreases bone turnover without impairing mineralization. *J Bone Miner Res* **14**:S1;SA378.

32. Goulet RW, Goldstein SA, Ciarelli MJ, Kuhn JL, Brown MB, Feldkamp LA 1994 The relationship between the structural and orthogonal compressive properties of trabecular bone. *J Biomech* **27**:375–389.
33. Thomsen JS, Ebbesen EN, Mosekilde L 1998 Relationships between static histomorphometry and bone strength measurements in human iliac crest bone biopsies. *Bone* **22**:153–163.
34. Ulrich D, Rietbergen van B, Laib A, Ruegsegger P 1999 The ability of three-dimensional structural indices to reflect mechanical aspects of trabecular bone. *Bone* **25**:55–60.
35. Chappard D, Legrand E, Basle MF, Fromont P, Racineux JL, Rebel A, Audran M 1996 Altered trabecular architecture induced by corticosteroids: A bone histomorphometric study. *J Bone Miner Res* **11**:676–685.
36. Currey J 1984 Bones, tendons, and muscles. In: *The Mechanical Adaptation of Bone*. Princeton University Press, Princeton, NJ, USA, pp. 185–222.
37. Bell GH, Dunbar O, Beck JS, Gibb A 1967 Variations in strength in vertebrae with age and their relation to osteoporosis. *Calcif Tissue Res* **1**:75–86.
38. Mosekilde L 1993 Vertebral structure and strength in vivo and in vitro. *Calcif Tissue Int* **53**(Suppl 1):S121–S126.
39. Borah B, Dufresne TE, Chmielewski PA, Prenger MC, Eriksen EF 2001 Risedronate (RIS) preserves bone architecture in osteoporotic postmenopausal women as measured by 3-D micro-computed tomography effects of bone turnover. *J Bone Miner Res* **16**:S1;S218.

Address reprint requests to:
Babul Borah, Ph.D.
Procter and Gamble Pharmaceuticals
8700 Mason-Montgomery Road
Mason, OH 45040, USA

Received in original form December 7, 2001; in revised form March 13, 2002; accepted April 16, 2002.